AGU PUBLICATIONS

Geophysical Research Letters

RESEARCH LETTER
10.1002/2016GL068182

Key Points:
- A plateau at the center of the Endeavour segment is underlain by thick crust
- The axial magmatic system in the lower crust is constrained to be no more than 10 km wide
- Decreased lower crustal velocities at the segment ends are likely due to hydrothermal alteration

Supporting Information:
- Supporting Information S1

Correspondence to:
D. Soule,
daxsoule@uw.edu

Citation:
Soule, D., W. S. D. Wilcock, D. R. Toomey, E. E. E. Hooft, and R. T. Weekly (2016), Near-axis crustal structure and thickness of the Endeavour Segment, Juan de Fuca Ridge, *Geophys. Res. Lett.*, *43*, 5688–5695, doi:10.1002/2016GL068182.

Received 15 FEB 2016
Accepted 3 MAY 2016
Accepted article online 13 MAY 2016
Published online 9 JUN 2016

Near-axis crustal structure and thickness of the Endeavour Segment, Juan de Fuca Ridge

Dax Soule[1], William S. D. Wilcock[1], Douglas R. Toomey[2], Emilie E. E. Hooft[2], and Robert T. Weekly[1,3]

[1]School of Oceanography, University of Washington, Seattle, Washington, USA, [2]Department of Geological Sciences, University of Oregon, Eugene, Oregon, USA, [3]Now at Incorporated Research Institutions for Seismology Data Management Center, Seattle, Washington, USA

Abstract A model of crustal thickness and lower crustal velocities is obtained for crustal ages of 0.1–1.2 Ma on the Endeavour Segment of the Juan de Fuca Ridge by inverting travel times of crustal paths and non-ridge-crossing wide-angle Moho reflections obtained from a three-dimensional tomographic experiment. The crust is thicker by 0.5–1 km beneath a 200 m high plateau that extends across the segment center. This feature is consistent with the influence of the proposed Heckle melt anomaly on the spreading center. The history of ridge propagation on the Cobb overlapping spreading center may also have influenced the formation of the plateau. The sharp boundaries of the plateau and crustal thickness anomaly suggest that melt transport is predominantly upward in the crust. Lower crustal velocities are lower at the ends of the segment, likely due to increased hydrothermal alteration in regions influenced by overlapping spreading centers, and possibly increased magmatic differentiation.

1. Introduction

At mid-ocean ridges, measurements of crustal thickness are an important tool for understanding the magmatic and volcanic processes that form oceanic crust. Among the geophysical tools available to estimate crustal thickness and structure, seismic tomography using crustal arrivals and Moho reflections (*Pg* and *PmP* phases, respectively) is well suited to distinguish variations in crustal thickness from variations in the seismic velocities of the lower crust. As such this method provides reliable constraints on magma flux from the mantle to crust, the composition and temperature of the lower crust, and by inference patterns of magma redistribution within the crust.

At the slow spreading Mid-Atlantic Ridge (MAR), both seismic [*Hooft et al.*, 2000; *Tolstoy et al.*, 1993; *Dunn et al.*, 2005] and gravity [*Lin et al.*, 1990; *Detrick et al.*, 1995] studies show that magmatic and volcanic accretion is spatially variable with the thickest crust found near the center of each ridge segment coincident with the shallowest bathymetry. The seismic images further show that crustal thickness variations result primarily from differences in lower crustal thickness [*Hooft et al.*, 2000; *Mutter and Mutter*, 1993; *Tolstoy et al.*, 1993]. These patterns are consistent with competing accretionary models, where either buoyant mantle flow [*Lin and Phipps Morgan*, 1992] or melt migration processes [*Magde and Sparks*, 1997] focus mantle-derived melt toward the segment center. Previous seismic studies also infer that some melt supplied to the segment centers is redistributed along axis in the upper crust by brittle diking events; however, to what degree the upper and lower crust at segment ends are formed by along-axis transport of magma, versus vertical delivery from the mantle, remains an open question [*Hooft et al.*, 2000; *Dunn et al.*, 2005; *Magde et al.*, 2000].

Along the fast spreading East Pacific Rise (EPR) at 8–10°N, melt delivery from the mantle to the crust is effectively continuous throughout tectonically defined ridge segments [*Toomey et al.*, 2007]. At the segment scale, the primary feature in crustal thickness maps is a broad band of thickened crust that forms behind the wake of the 9°03′ overlapping spreading center (OSC) [*Canales et al.*, 2003]. Between tectonic offsets, centers of melt delivery from the mantle to the crust are spaced at intervals of ~25 km [*Toomey et al.*, 2007], effectively defining volcanic or third-order segmentation of the ridge. Seismic studies of the mantle, lower crust, and midcrustal axial magma chamber all conclude that along-axis transport of melt at mantle or crustal depths is unlikely at the scale of a tectonically defined ridge segment. To what degree melt is redistributed at the scale of third-order or volcanic-scale segmentation is unknown, although detailed studies of the AMC reflector near 9°50′N suggest that vertical

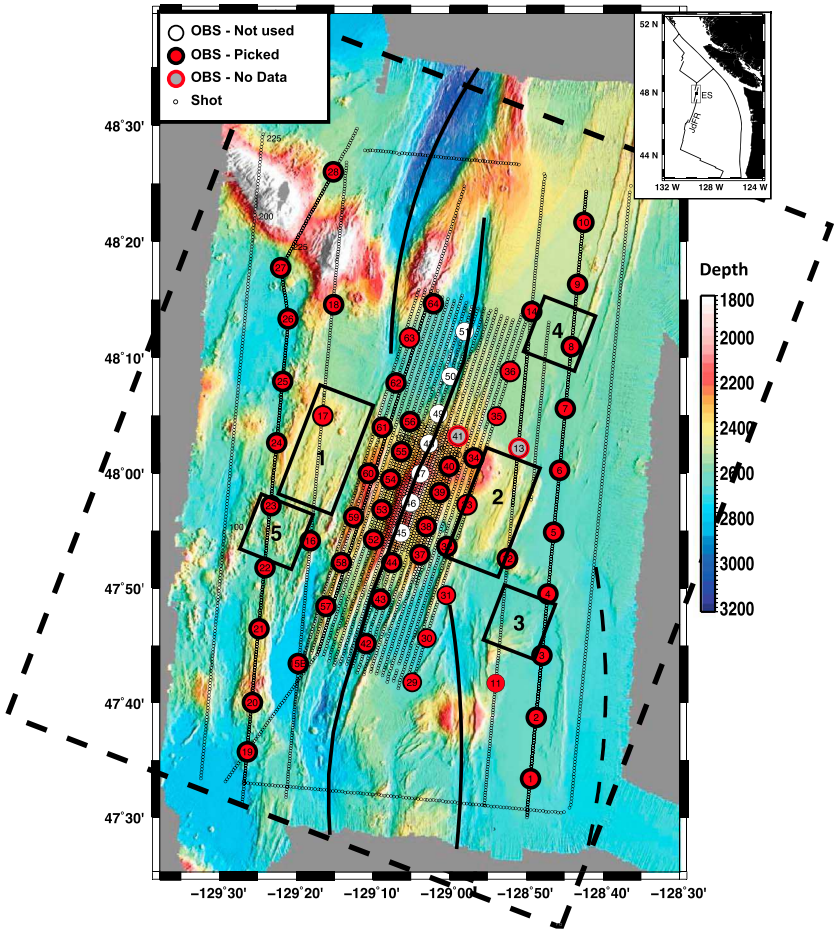

Figure 1. Bathymetric map of the Endeavour Segment of the Juan de Fuca Ridge showing the configuration of the tomography experiment with shots shown as small open circles and OBSs as large circles labeled with the site number and colored red for OBSs used in this study, white for OBS not used, and grey for OBSs that did not return data. The dashed box shows the bounds of the *X-Y* grid used for the inversions. The locations of plate boundaries (solid lines), a relict propagating rift of the Cobb OSC (dashed line) and five numbered boxes that bound areas used to calculate average crustal velocities in Figure 2, are also shown. Areas 1 and 2 cover off-axis portions of central Endeavour plateau on the Pacific and Juan de Fuca plates, respectively, area 3 overlies an area impacted by the Cobb OSC, and areas 4 and 5 are representative areas of crust off the plateau on the Pacific and Juan de Fuca plates, respectively. The inset figure shows the location of the study area in relation to the coast of the Pacific Northwest and plate boundaries with labels as follows: JdFR, Juan de Fuca Ridge, ES, Endeavour Segment.

transport of melt in the lower crust likely resupplies the upper crustal magma chamber [*Aghaei et al.*, 2014; *Carbotte et al.*, 2013].

In this paper, we use seismic tomography to examine the variations in off-axis crustal thickness and lower crustal velocity at the Endeavour segment of the Juan de Fuca Ridge (Figure 1). This is an intermediate spreading-rate ridge which has some characteristics of both slow and fast spreading ridges. The central portion of the ridge is underlain by a midcrustal magma chamber similar to that seen at the EPR [*Van Ark et al.*, 2007]. Somewhat like the MAR although more muted, there are variations in elevation along the spreading axis; the segment center comprises a plateau which extends out to crustal ages of ~0.71 Ma and is elevated ~200 m relative to adjacent regions [*Carbotte et al.*, 2008]. The segment is bounded by OSCs that are similar to those seen on the EPR. Althoug there is a considerable amount of melt stored at mantle depths beneath the OSCs [*VanderBeek et al.*, 2016], the limbs are not in most places underlain by a crustal magma chamber [*Carbotte et al.*, 2006; *Van Ark et al.*, 2007]. Along-axis variations in upper crustal structure show similarities to both the MAR and EPR [*Weekly et al.*, 2014]. The Endeavour, thus, represents a good site to further investigate the roles of axial magmatic systems and ridge segmentation in shaping the volcanic structure of oceanic crust.

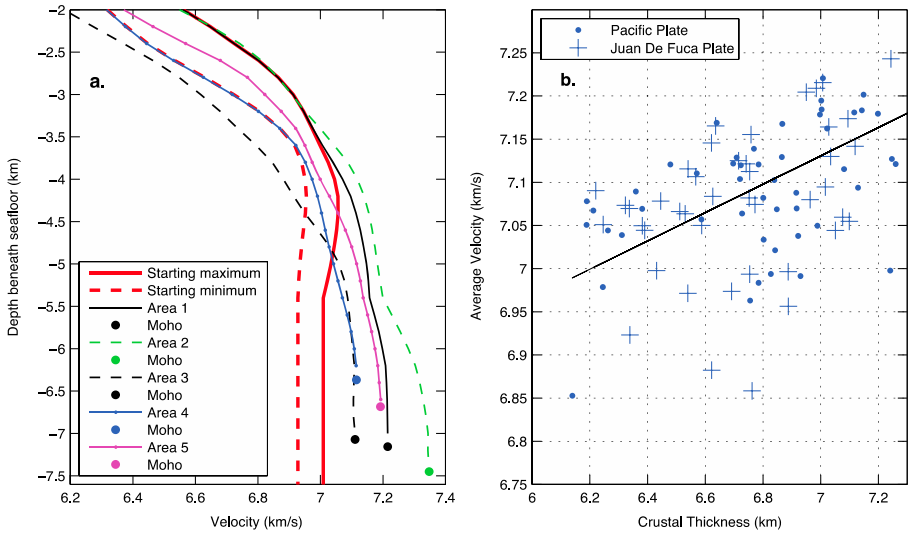

Figure 2. (a) Vertical velocity profiles for the middle to lower crust showing the minimum and maximum velocities in the starting model (bold red dashed and solid lines, respectively) and horizontal averaged velocity in the preferred model for areas 1 (black solid), 2 (green dashed), 3 (faint black dashed), 4 (blue solid with dots), and 5 (magenta solid with dots) (see Figure 1). These profiles have gradients that are pretty typical for normal oceanic crust. Mean crustal thickness in each area which are 7.2 km for area 1, 7.5 km for area 2, 7.1 km for area 3, 6.4 km for area 4 and 6.7 km for area 5 are also shown by terminal dots. (b) Average velocity over the lower 2 km of crust plotted versus crustal thickness for the Pacific plate (dots) and Juan de Fuca plate (pluses). Averages were obtained for 5 km by 5 km grid squares and are limited to regions with ray coverage ≥10 km from the spreading axis. There is a noticeable positive correlation between lower crustal velocities and crustal thickness (black line, $R^2 = 0.4$).

2. Experiment and Method

In 2009 we conducted a seismic tomography experiment on the Endeavour segment of the Juan de Fuca Ridge using 64 ocean bottom seismographs (OBSs) to record ~5500 air gun shots from the 36-element, 108154.6 cm^3 array of the R/V *Marcus G. Langseth* (Figure 1). *Weekly et al.* [2014] inverted 93,000 crustal *P* wave (*Pg*) arrivals for the segment-scale isotropic and anisotropic velocity structure of the upper oceanic crust. The models are characterized by low velocities at the segment ends relative to the segment center that were interpreted in terms of increased fracturing in the upper crust created near the OSCs and possibly less hydrothermal infilling of porosity. More recently *Morgan et al.* [2016] have used full-waveform inversions to improve the resolution of shallow upper crustal structure in the central portion of the experiment footprint.

In this study, the goal is characterize lower crustal structure and thickness off axis using wide-angle, Moho-reflected *P* wave arrivals (*PmP*); future work will expand these models to the ridge axis where axial crustal magma bodies complicate the analysis. Approximately 19,000 *PmP* arrival times were iteratively handpicked for non-ridge-crossing paths with reflection points at crustal ages of 0.1–1.2 Ma. Uncertainties were visually estimated on the basis of the signal-to-noise ratio and trace-to-trace coherency. In Text S1 and Figures S1–S3 in the supporting information, we provide details of our process for picking *PmP* arrivals and show examples of record sections with *PmP* picks.

The starting velocity model for our inversion is a three-dimensional isotropic model obtained by inverting the *Pg* data set of *Weekly et al.* [2014]; to obtain this starting model we used an inversion strategy similar to theirs, except that we do not include the effects of upper crustal anisotropy and we use a creeping strategy as opposed to jumping [*Shaw and Orcutt*, 1985]. The results of this creeping inversion yield an upper crustal model, in which all signal that can be attributed to upper crustal structure has been accounted for prior to inverting for lower crustal structure. Velocities in this model at 5.6 km depth, the largest depth sampled anywhere by *Pg* in the model of *Weekly et al.* [2014], are extended downward to create a starting model for the *PmP* inversion (Figure 2a). A Moho interface is draped from a smoothed version of the seafloor at 6.8 km depth. The *Pg* and *PmP* arrivals were then inverted jointly using the method of *Dunn et al.* [2005] and a jumping strategy [*Shaw and Orcutt*, 1985]. Including the *Pg* arrival times ensures that the inversion

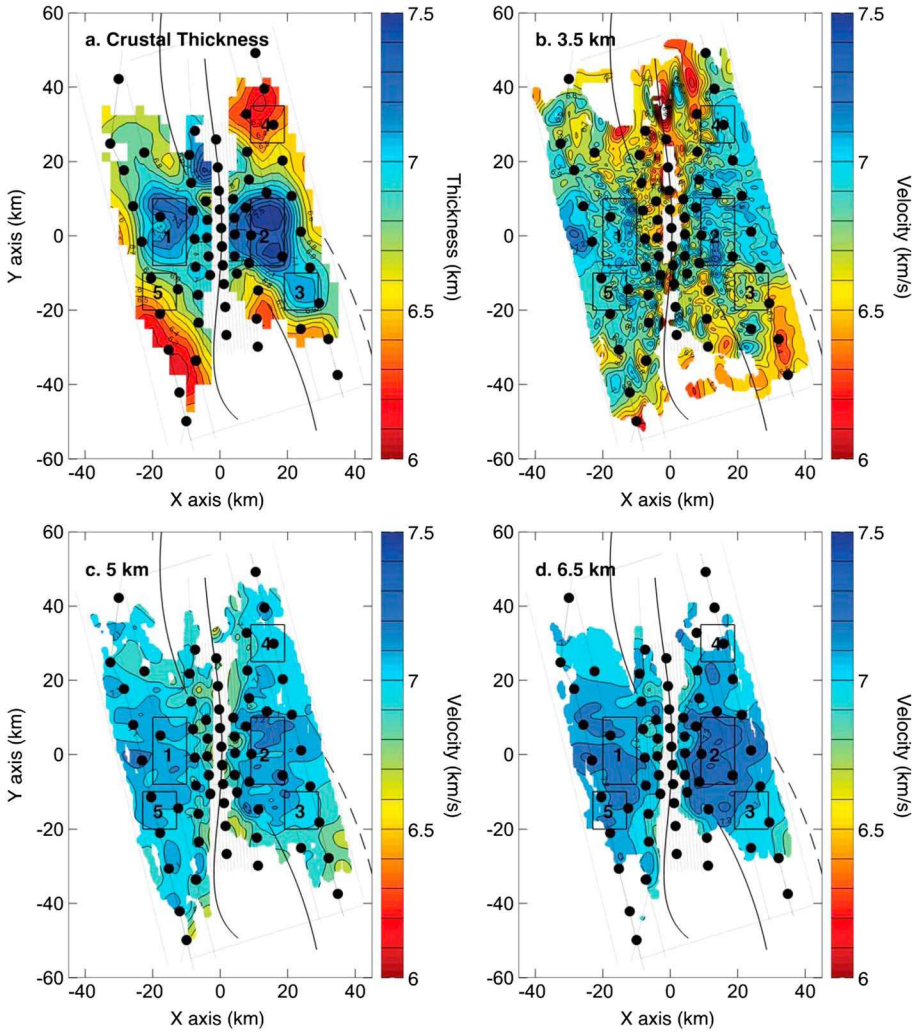

Figure 3. Contour plots showing (a) crustal thickness and crustal velocity at (b) 3.5 km, (c) 5 km, and (D) 6.5 km depth for the preferred inversion with masking in regions with no ray coverage. The plate boundaries (solid black lines), the relict propagator (dashed black line), the locations of OBSs (filled black circles) and shots (dots), and the five areas used to calculate the averaged vertical profiles shown in Figure 2 (numbered boxes) are also shown.

retains the upper crustal structure required by the *Pg* data, while the *PmP* arrival times constrain the lower crustal velocity and crustal thickness

The inverse method [*Dunn et al.*, 2005] iteratively solves for perturbations to the starting crustal isotropic slowness and crustal thickness model by minimizing the variance of the travel time misfit and imposing smoothing and dampening terms with user-defined weights. We used perturbational nodes for slowness of 1 km and 0.25 km in the horizontal and vertical directions, respectively, and 2.5 km on the Moho interface. We systematically explored different choices of smoothing parameters to find the smoothest model with an acceptable fit to the travel time data and employed inversions of synthetic data to demonstrate that the primary features are well resolved. Our preferred model fits the data to its uncertainties (see Figure S4) and is insensitive to the starting model (see Figure S5).

3. Results

Figure 3 shows maps of crustal thickness and lower crustal velocity anomalies obtained from tomographic inversion of *Pg* and *PmP* data. The mean crustal thickness in resolved regions is 6.8 km, and the range is 5.9 km–7.7 km. The most prominent feature of the model is a region of thicker crust beneath the central

Endeavour that coincides with the bathymetric plateau (Figure 3a, areas 1 and 2). In addition, crust is thicker in smaller regions to the southeast of the plateau (area 3) and to the north just west of the Endeavour Ridge.

The boundaries of the thicker crust, in the center of the segment, correspond closely with edges of the bathymetric plateau; while wide-angle reflections do not have good horizontal resolution, modeling that tested the sensitivity of the inversion to the sharpness of the transition suggest that the data are consistent with a sharp transition in crustal thickness at the edges of the plateau (see Figures S6–S8). Well off-axis, the average crustal thickness beneath the plateau (areas 1 and 2 on Figure 2a) is ~0.5–1 km greater than adjacent sites away from the plateau (areas 4 and 5). Crustal thickness beneath the plateau is asymmetric; the thickness on the Juan de Fuca plate is about 0.3 km greater than on the Pacific plate. In addition, there appears to be a decrease in crustal thickness beneath the plateau toward the ridge axis.

Lower crustal velocities are not imaged directly beneath the ridge axis but are depressed in a band that extends about 3–5 km to either side (Figures 3b–3d). As for the upper crust [*Weekly et al.*, 2014], velocities in the lower crust are elevated in the segment center in an area that includes the bathymetric plateau and extends about 10 km to the south. Average velocities in the segment center (areas 1 and 2 on Figure 2a) are ~0.15 km/s higher than those found near the segment ends (area 4). This leads to a noticeable correlation between lower crustal velocities and crustal thickness (Figure 2b). Lower crustal velocities are also slightly asymmetric across the central Endeavour with average velocities ~0.1 km/s higher on the Juan de Fuca plate. The correlation between crustal thickness and lower crustal velocity beneath the plateau is the opposite of what would be expected if the inversion mapped some of the increased *PmP* travel times from thicker crust into velocity; synthetic inversions confirm that there is little trade-off between crustal thickness and velocity in this region (see Figures S6–S8).

4. Discussion

The observation of thicker crust beneath the plateau is consistent with the results of *Carbotte et al.* [2008], who estimated a similar crustal thickness increase beneath the plateau from the analysis of vertically incident Moho reflections in a multichannel seismic profile. However, unlike this earlier study, we see no evidence for thicker crust extending beyond the western limit of the plateau toward the Heckle seamount chain. As reported by *Carbotte et al.* [2008], the crustal thicknesses are consistent with the central plateau being isostatically supported by a thicker crust. For example, assuming a lower crustal density of 2950 kg m^{-3} [*Carlson and Miller*, 2004] and a mantle density of 3300 kg m^{-3} [*McKenzie et al.*, 2005], the ~200 m high plateau would be isostatically compensated by an increase in lower crustal thickness of ~1.1 km [e.g., *Turcotte and Schubert*, 2002]. This is a reasonable match to the upper limit of the observed crustal thickening but given the uncertainties in parameters, the seismic data cannot rule out an isostatic contribution from crustal density changes [e.g., *Toomey and Hooft*, 2008].

Carbotte et al. [2008] attribute the thicker crust beneath the plateau to enhanced mantle melt production resulting from the Juan de Fuca Ridge overriding the melting anomaly that created the Heckle Seamount chain. They note that the onset of thicker crust at 0.71 Ma coincided with a lengthening of the Endeavour segment and a temporary reversal of the long-term northward propagation of the Cobb OSC. The sharp western and eastern boundaries of the plateau and the absence of thicker crust west of the plateau imply that the Heckle melt anomaly transitioned quickly from supporting the growth of off-axis seamounts to feeding the spreading center.

If the plateau is the result of a Heckle melting anomaly, our data suggest that the influence of the anomaly is waning because crustal thickness beneath the plateau decreases substantially toward the ridge axis. Our inversion excludes *PmP* travel times for ridge crossing paths, which reduces the number of Moho reflections near the ridge axis, but synthetic inversions with the same ray geometry and travel times based on a uniform thickness crust beneath the plateau, show only a small decrease in apparent crustal thickness toward the ridge axis (Figure S8a) suggesting that the observed crustal thinning is not an artifact of uneven ray coverage. *Carbotte et al.* [2008] suggest that renewed northward propagation of the Cobb OSC in the past 100,000 years as the Northern Symmetric Segment lengthens [*Johnson et al.*, 1983; *Shoberg et al.*, 1991] is consistent with a waning influence of the Heckle melt anomaly. In addition, the chemistry of basalts along the Endeavour has been interpreted in terms of a failing rift that is underlain by diminishing mantle melting [*Karsten et al.*, 1986]. Our results are consistent with these interpretations, but other interpretations are possible, as discussed below.

It is difficult to explain the across-axis asymmetry in crustal thickness beneath the plateau in terms of the migration of the Heckle melt anomaly. The westward migration of the spreading axis toward a mantle heterogeneity is predicted to produce increased melting beneath the Pacific plate [*Davis and Karsten*, 1986]. *Carbotte et al.* [2008] identify a small recent eastward jump of the Endeavour spreading axis based on across-axis asymmetry in the width of the Brunhes magnetic anomaly, which they interpret as evidence that the Heckle melt anomaly has moved east of the ridge axis. However, this is a recent event and the asymmetry in crustal thickness is most pronounced on the outer flanks of the plateau.

It is possible that the asymmetry reflects across axis differences in the structure of the Moho. If the Moho transition zone is thicker beneath the Pacific Plate and first-arriving *PmP* picks tend to be for reflection near the top of the transition zone then the crustal thicknesses may be biased shallower beneath the Pacific plate. The *PmP* arrivals are harder to pick for paths on the Pacific Plate, and the RMS travel time residuals for the inversion are markedly larger for paths traversing area 1 than area 2 (23.5 ms versus 18.2 ms; Figures S4f and S4h). This might indicate that the Moho structure is more complex beneath the Pacific side of the plateau.

Alternatively, the propagation history of the Cobb OSC may have led to the formation of an asymmetric plateau. *VanderBeek et al.* [2016] argue that the advancing limb of an OSC taps melt that ponds beneath the overlap basin, leading to thickened crust in its wake. At the Endeavour, the onset time and position of the plateau coincide with the northernmost advance of the North Symmetric segment prior to the Brunhes-Matuyama reversal [*Carbotte et al.*, 2008] (Figure 1). According to this model the subsequent southward growth of the Endeavour segment would have generated thicker crust in the vicinity of the plateau by tapping mantle melt that was asymmetrically concentrated beneath the Juan de Fuca Plate. This mechanism could have acted in concert with the capture of the Heckle melt anomaly. However, we note that *Dziak* [2006] argue that the seamount chains to the west of the Endeavour coincide with strike-slip faults associated with southward reorganization of the Juan-de-Fuca/Pacific/North American triple junction, an explanation that does not require that the Heckle seamount chain results from a small melting anomaly fixed within the mantle reference frame. Thus, it is possible to produce chains of seamounts and a near-axis bathymetric plateau without invoking a mantle melt anomaly.

The characteristics of the plateau support a model in which along-axis melt transport is inefficient in the lower crust. The axial magma chamber that is present at the segment center can presumably feed diking events that propagate to the segment ends [*Van Ark et al.*, 2007], and there is evidence of recent diking events on the northern Endeavour propagating southward, presumably in the upper to midcrust, from a melt source near Endeavour Seamount [*Hooft et al.*, 2010; *Weekly et al.*, 2013]. However, the sharp northern and southern edges of the plateau and of the crustal thickness variations that appear to support it isostatically suggest the temperatures of the lower crust away from the plateau are insufficient for ductile flow to transfer lower crustal material to the segment ends. On the basis of our results, we infer that melt transport at lower crustal levels is predominantly in the vertical direction. Similar inferences have been made for both the Mid-Atlantic Ridge [*Hooft et al.*, 2000] and the East Pacific Rise [*Carbotte et al.*, 2013].

The near- and off-axis lower crustal velocity model is consistent with the results from the EPR, which show that the axial magmatic system in the lower crust solidifies and cools within a few kilometers of the ridge axis [*Dunn et al.*, 2000]. Although our velocity model does not extend to the ridge axis, velocities generally decrease toward the ridge by about 0.2 km/s, relative to velocities at a distance of ~5 km off-axis. This imaged velocity anomaly can be explained by a temperature change of ~200°C [*Christensen*, 1979], relative to lower crustal temperatures well off axis. Thus, while we have not imaged the axial magmatic system, we can infer that its cross-axis width is less than 10 km.

Ridge-parallel velocity variations in the lower crust well off-axis may be related to variations in hydrothermal alteration. *Weekly et al.* [2014] interpreted lower velocities in the upper and middle crust at the segment ends in terms of increased porosity due to enhanced fracturing associated with deformation in the overlapping spreading centers. It is unlikely that porosity can explain the lower crustal velocity variations; a porosity change approaching 1% is required generate the observed velocity variation of 0.15 km/s but the overburden pressure in the lower crust likely limits maximum porosities to $<$0.5% [*Carlson and Herrick*, 1990; *Iturrino et al.*, 1991]. A more likely explanation is that the presence or absence of talc and/or serpentine in the microcracks of olivine crystals has a substantial effect on the elastic properties of Gabbro [*Carlson et al.*, 2009]. Thus, the lower velocities at the segment ends are likely a result of enhanced hydrothermal alteration promoted by

increased fracturing of the upper crust. Likewise, at the segment center the velocities we observe are higher than 7 km/s, which may indicate that alteration is less than typical for lower crustal gabbros [*Carlson and Miller*, 2004].

An alternative explanation for the higher lower crustal velocities near the segment center is that they are related to compositional variations [*Toomey and Hooft*, 2008]. If the lower crust near the segment center has undergone less differentiation than at the segment ends it will have higher velocities [*Iturrino et al.*, 1991]. It will also have lower densities that might contribute to the isostatic compensation of the plateau. We note that at the Lau back arc basin, *Arai and Dunn* [2014] also observe a positive correlation between lower crustal velocity and crustal thickness which they attribute to variable influences of water released from the subducting slab. However, the slope of their fit is larger from ours (~0.4 s^{-1} versus ~0.15 s^{-1}), which supports a different causative mechanism.

Two smaller areas of thicker crust are also present within our model. The first connects to the southeast corner of the plateau and coincides with a region of disturbed topography that formed during the northward propagation of the Northern Symmetric segment prior the Brunhes-Matuyama reversal [*Carbotte et al.*, 2008]. It may thus be a region of crustal thickening that formed behind the tip of the propagator [*Canales et al.*, 2003; *Marjanović et al.*, 2011; *VanderBeek et al.*, 2016]. Crustal velocities in this region are relatively low, which is consistent with a region of differentiated magmas as is often observed near propagating ridge tips [e.g., *Sempere et al.*, 1984].

The second smaller area of thicker crust lies within the overlap basin of the West-Valley Endeavour OSC and is immediately north of a region of thin crust near the spreading axis that cuts into the plateau. The thin crust coincides with a region of intense ongoing seismicity that is interpreted as a region of extension at the southernmost limit of the West Valley propagator [*Weekly et al.*, 2013]. The thicker crust to the north is harder to explain—it is beneath the advancing part of the overlap basin rather than behind it as the OSC models predict [*Marjanović et al.*, 2011; *VanderBeek et al.*, 2016] and is south of the region of enhanced mantle melt concentrations imaged beneath the center of the OSC [*VanderBeek et al.*, 2016].

5. Conclusions

We present the results of a tomographic inversion for crustal thickness and lower crustal velocities on the Endeavour segment of the Juan de Fuca Ridge using Moho reflections for paths that do not cross the ridge axis. Our results confirm that a 200 m high bathymetric plateau extending out to crustal ages of 0.71 Ma is underlain by a region of crust that is thicker by 0.5–1.0 km with higher apparent thicknesses on the east flank. The crustal thickness increases may be sufficient to support the plateau isostatically but the seismic data cannot rule out a contribution from crustal density variations. The symmetric component of crustal thickness beneath the plateau can be explained by the spreading center overriding the Heckle melting anomaly [*Carbotte et al.*, 2008]. Alternatively, the asymmetry and perhaps some of the symmetric component may result from the history of ridge propagation in the Cobb OSC [*VanderBeek et al.*, 2016]. The sharp boundaries of the plateau suggest that the lower crust is too cool near the segment ends for ductile flow to even out crustal thickness and that melt transport within the crust is primarily vertical as previously inferred at the Mid-Atlantic Ridge and East Pacific Rise. Gradients in crustal velocity near the ridge axis suggest that the axial magmatic system cools within a few kilometers of the ridge axis as is observed at the EPR [*Dunn et al.*, 2000]. Depressed lower crustal velocities in crust created at the ends of the segment are most likely a result of a combination of enhanced hydrothermal alteration and compositions that are more differentiated.

Acknowledgments

The data used in this research were collected using instruments from the U.S. Ocean Bottom Seismograph Instrument Pool and are archived at the IRIS Data Management Center (www.iris.edu). We thank the officers, crew, and marine technicians of the R/V *Marcus G. Langseth*, the OBS teams from Scripps Institution of Oceanography and Woods Hole Oceanographic Institution, and passive acoustic technicians and marine mammal observers for their assistance at sea in the acquisition of the seismic data. We thank Pablo Canales and Richard Carlson for their constructive reviews of the manuscript. The experiment and analysis were supported by the NSF under grants OCE- 0454700 to the University of Washington and OCE-0454747 and OCE-0651123 to the University of Oregon.

References

Aghaei, O., M. R. Nedimović, H. Carton, S. M. Carbotte, J. P. Canales, and J. C. Mutter (2014), Crustal thickness and Moho character of the fast-spreading East Pacific Rise from 9°42′N to 9°57′N from poststack-migrated 3-D MCS data, *Geochem. Geophys. Geosyst.*, *15*, 634–657, doi:10.1002/2013GC005069.

Arai, R., and R. A. Dunn (2014), Seismological study of Lau back arc crust: Mantle water, magmatic differentiation, and a compositionally zoned basin, *Earth Planet. Sci. Lett.*, *390*, 304–317, doi:10.1016/j.espl.2014.01.014.

Canales, P. J., R. S. Detrick, D. R. Toomey, and W. S. D. Wilcock (2003), Segment-scale variations in the crustal structure of 150–300 kyr old fast spreading oceanic crust (East Pacific Rise, 8°15′N–10°5′N) from wide-angle seismic refraction profiles, *Geophys. J. Int.*, *152*, 766–794, doi:10.1046/j.1365-246X.2003.01885.x.

Carbotte, S. M., R. S. Detrick, A. Harding, J. P. Canales, J. Babcock, G. Kent, E. Van Ark, M. Marjanović, and J. Diebold (2006), Rift topography linked to magmatism at the intermediate spreading Juan de Fuca Ridge, *Geol. Soc. Am. Bull.*, *34*, 209–212, doi:10.1130/G21969.1.

Carbotte, S. M., M. R. Nedimović, J. P. Canales, G. M. Kent, A. J. Harding, and M. Marjanović (2008), Variable crustal structure along the Juan de Fuca Ridge: Influence of on-axis hot spots and absolute plate motions, *Geochem. Geophys. Geosyst*, *9*, Q08001, doi:10.1029/2007GC001922.
Carbotte, S. M., M. Marjanović, M. Helene, J. C. Mutter, J. P. Canales, M. R. Nedimović, S. S. Han, and M. R. Perfit (2013), Fine-scale segmentation of the crustal magma beneath the East Pacific Rise, *Nat. Geosci.*, *6*, 866–870, doi:10.1038/ngeo1933.
Carlson, R. L., and C. N. Herrick (1990), Densities and porosities in the oceanic crust and their variations with depth and age, *J. Geophys. Res.*, *95*, 9153–9170, doi:10.1029/JB095iB06p09153.
Carlson, R. L., and J. D. Miller (2004), Influence of pressure and mineralogy on seismic velocities in ocean gabbros: Implications for the composition and state of the lower crust, *J. Geophys. Res.*, *109*, B09205, doi:10.1029/2003JB002699.
Carlson, R. L., J. D. Miller, and J. Newman (2009), Olivine enigma: Why alteration controls the seismic properties of oceanic gabbros, *Geochem. Geophys. Geosyst.*, *10*, Q03O16, doi:10.1029/2008GC002263.
Christensen, N. I. (1979), Compressional wave velocities in rocks at high temperatures and pressures, critical thermal gradients, and crustal low-velocity zones, *J. Geophys. Res.*, *84*, 6849–6857, doi:10.1029/JB084iB12p06849.
Davis, E. E., and J. L. Karsten (1986), On the cause of the asymmetric distribution of seamounts about the Juan de Fuca ridge: Ridge-crest migration of a heterogeneous asthenosphere, *Earth Planet. Sci. Lett.*, *79*(3–4), 385–396, doi:10.1016/0012-821X(86)90194-9.
Detrick, R. S., H. D. Needham, and V. Renard (1995), Gravity anomalies and crustal thickness variations along the Mid-Atlantic Ridge between 33°N and 40°N, *J. Geophys. Res.*, *100*, 3767–3787, doi:10.1029/94JB02649.
Dunn, R. A., D. R. Toomey, and S. C. Solomon (2000), Three-dimensional seismic structure and physical properties of the crust and shallow mantle beneath the East Pacific Rise at 9°30′N, *J. Geophys. Res.*, *105*, 23,537–23,555, doi:10.1029/2000JB900210.
Dunn, R. A., V. Lekić, R. S. Detrick, and D. R. Toomey (2005), Three-dimensional seismic structure of the Mid-Atlantic Ridge (35°N): Evidence for focused melt supply and lower crustal dike injection, *J. Geophys. Res.*, *110*, B09101, doi:10.1029/2004JB003473.
Dziak, R. P. (2006), Explorer deformation zone and reorganization of the Pacific-Juan de Fuca-North American tripple junction, *Geology*, *34*(3), 213–216, doi:10.1130/G22164.1.
Hooft, E. E. E., R. S. Detrick, D. R. Toomey, J. A. Collins, and J. Lin (2000), Crustal thickness and structure along three contrasting spreading segments of the Mid-Atlantic Ridge, 33.5°–35°N, *J. Geophys. Res.*, *105*, 8205–8226, doi:10.1029/1999JB900442.
Hooft, E. E. E., et al. (2010), A seismic swarm and regional hydrothermal and hydrologic perturbations: The northern Endeavour segment February 2005, *Geochem. Geophys. Geosyst*, *11*, Q12015, doi:10.1029/2010GC003264.
Johnson, H. P., J. L. Karsten, J. R. Delaney, E. E. Davis, R. G. Currie, and R. L. Chase (1983), A detailed study of the Cobb Offset of the Juan de Fuca Ridge: Evolution of a propagating rift, *J. Geophys. Res.*, *88*, 2297–2315, doi:10.1029/JB088iB03p02297.
Iturrino, G. J., N. I. Christensen, S. Kirby, and M. H. Salisbury (1991), Seismic velocities and elastic properties of oceanic gabbroic rocks from hole 735B, *Proc. Ocean Drill. Prog. Sci. Results.*, *118*, 227–244, doi:10.2973/odp.proc.sr.118.151.1991.
Karsten, J. L., S. R. Hammond, E. E. Davis, and R. G. Currie (1986), Detailed geomorphology and neotectonics of the Endeavour Segment, Juan de Fuca Ridge: New results from Seabeam swath mapping, *Geo. Soc. Am. Bul.*, *97*(2), 213–221, doi:10.1130/0016-7606(1986)97<213:DGANOT>2.0.CO;2.
Lin, J., and J. Phipps Morgan (1992), The spreading rate dependence of 3-dimensional mid-ocean ridge gravity structure, *J. Geophys. Res. Lett.*, *19*(1), 13–16, doi:10.1029/91GL03041.
Lin, J., G. M. Purdy, H. Schouten, J. C. Sempere, and C. Zervas (1990), Evidence from gravity data for focused magmatic accretion along the Mid-Atlantic Ridge, *Nature*, *344*, 627–632, doi:10.1038/344627a0.
Magde, L. S., and D. W. Sparks (1997), Three-dimensional mantle upwelling, melt generation, and melt migration beneath segment slow spreading ridges, *J. Geophys. Res.*, *102*, 20,571–20,583, doi:10.1029/97JB01278.
Magde, L. S., A. H. Barclay, D. R. Tommey, R. S. Detrick, and J. A. Collins (2000), Crustal magma plumbing within a segment of the Mid-Atlantic Ridge, 35°N, *Earth Planet. Sci. Lett.*, *175*(1–2), 55–67, doi:10.1016/S0012-821X(99)00281-2.
Marjanović, M., S. M. Carbotte, M. R. Nedimović, and J. P. Canales (2011), Gravity and seismic study of crustal structure along the Juan de Fuca Ridge axis and across pseudofaults on the ridge flanks, *Geochem. Geophys. Geosyst.*, *12*, Q05008, doi:10.1029/2010GC003439.
McKenzie, D., J. Jackson, and K. Priestley (2005), Thermal structure of oceanic and continental lithosphere, *Earth Planet. Sci. Lett.*, *223*, 337–349, doi:10.1016/j.epsl.2005.02.005.
Morgan, J., M. Warner, G. Arnoux, E. E. E. Hooft, D. R. Toomey, B. VanderBeek, and W. S. D. Wilcock (2016), Next-generation seismic experiments – II: Wide-angle, multi-azimuth, 3-D, full-waveform inversion of sparse field data, *Geophys. J. Int.*, *204*, 1342–1363, doi:10.1093/gji/ggv513.
Mutter, C. Z., and J. C. Mutter (1993), Variations in thickness of layer 3 dominate oceanic crustal structure, *Earth Planet. Sci. Lett.*, *117*, 295–317, doi:10.1016/0012-821X(93)90134-U.
Sempere, J. C., K. C. Macdonald, and S. P. Miller (1984), Overlapping spreading centres: 3-D inversion of the magnetic field at 9°03′N on the East Pacific Rise, *Geophys. J. Roy. Astron. Soc.*, *79*, 799–811, doi:10.1111/j.1365-246X.1984.tb02869.x.
Shaw, P. R., and J. A. Orcutt (1985), Waveform inversion of seismic refraction data and applications to young Pacific crust, *Geophys. J. R. Astron. Soc.*, *82*, 375–414, doi:10.1111/j.1365-246X.1985.tb05143x.
Shoberg, T., S. Stein, and J. Karsten (1991), Constraints on rift propogation history at the Cobb offset, Juan de Fuca Ridge, from numerical modeling of tectonic fabric, *Tectonophysics*, *197*, 295–308, doi:10.1016/0040-1951(91)90047-V.
Tolstoy, M., A. J. Harding, and J. A. Orcutt (1993), Crustal thickness on the Mid-Atlantic Ridge: Bull's-eye gravity anomalies and focused accretion, *Science*, *262*, 726–729, doi:10.1126/science.262.5134.726.
Toomey, D. R., and E. E. E. Hooft (2008), Mantle upwelling, magmatic differentiation, and the meaning of axial depth at fast-spreading ridges, *Geology*, *36*(9), 679–682, doi:10.1130/G24834A.1.
Toomey, D. R., D. Jousselin, R. A. Dunn, W. S. D. Wilcock, and R. S. Detrick (2007), Skew of mantle upwelling beneath the East Pacific Rise governs segmentation, *Nature*, *446*, 409–414, doi:10.1038/nature05679.
Turcotte, D., and G. Schubert (2002), *Geodynamics*, 2nd ed., 219 pp., Cambridge Univ. Press, New York.
Van Ark, E. M., R. S. Detrick, J. P. Canales, S. M. Carbotte, A. J. Harding, G. M. Kent, M. R. Nedimovic, W. S. D. Wilcock, J. B. Diebold, and J. M. Babcock (2007), Seismic structure of the Endeavour Segment, Juan de Fuca Ridge: Correlations with seismicity and hydrothermal activity, *J. Geophys. Res.*, *112*, B02401, doi:10.1029/2005JB004210.
VanderBeek, B., D. R. Toomey, E. E. E. Hooft, and W. S. D. Wilcock (2016), Segmentation of mid-ocean ridges caused by oblique mantle divergence, *Nature Geosci.*, in press.
Weekly, R. T., W. S. D. Wilcock, E. E. E. Hooft, D. R. Toomey, P. R. McGill, and D. S. Stakes (2013), Termination of a 6 year ridge-spreading event observed using a seafloor seismic network on the Endeavour Segment, Juan de Fuca Ridge, *Geochem. Geophys. Geosyst.*, *14*, 1375–1398, doi:10.1002/ggge.20105.
Weekly, R. T., W. S. D. Wilcock, D. R. Toomey, E. E. E. Hooft, and E. Kim (2014), Upper crustal seismic structure of the Endeavour segment, Juan de Fuca Ridge from travel time tomography: Implications for oceanic crustal accretion, *Geochem. Geophys. Geosyst.*, *15*, 1296–1315, doi:10.1002/2013GC005159.